An Animal Model for Cystic Fibrosis Made by Gene Targeting

John N. Snouwaert, Kristen K. Brigman, Anne M. Latour,
Nadia N. Malouf, Richard C. Boucher, Oliver Smithies,
Beverly H. Koller*

Cystic fibrosis results from defects in the gene encoding a cyclic adenosine monophosphate–dependent chloride ion channel known as the cystic fibrosis transmembrane conductance regulator (CFTR). To create an animal model for cystic fibrosis, mice were generated from embryonic stem cells in which the CFTR gene was disrupted by gene targeting. Mice homozygous for the disrupted gene display many features common to young human cystic fibrosis patients, including failure to thrive, meconium ileus, alteration of mucous and serous glands, and obstruction of glandlike structures with inspissated eosinophilic material. Death resulting from intestinal obstruction usually occurs before 40 days of age.

Cystic fibrosis (CF) is the most common potentially lethal autosomal recessive disorder in Caucasian populations and affects about 1 of every 2500 newborns; the frequency of heterozygous carriers has been estimated at about 5 percent. The protein product that is defective or absent in CF patients is a cyclic AMP–regulated chloride ion channel called the cystic fibrosis transmembrane conductance regulator (CFTR) (1, 2). In addition to its role as a chloride channel, the CFTR protein has been reported to regulate cyclic AMP–dependent endocytosis and exocytosis in epithelial cells (3, 4). In patients with CF, more than 170 different mutations have been described in the CFTR gene (5) although the deletion of three bases in exon 10 (ΔF508) is responsible for 70 percent of all CF mutations (6).

The predominant symptoms of CF can be attributed to abnormalities of epithelial surfaces in the respiratory, digestive, and reproductive tracts. About 85 percent of individuals with CF show pancreatic exocrine insufficiency, while 10 percent of newborns with CF suffer from meconium ileus, an intestinal obstruction caused by viscous, putty-like meconium. Other symptoms include cirrhosis of the liver and infertility, especially in males. Before the development of effective treatments, pancreatic and intestinal complications were among the chief causes of death among CF patients. Today, however, death usually occurs as a result of respiratory infection

that follows obstruction of the airways by thick, viscous mucus (7).

Many of the pathological changes seen in CF patients can be attributed to the presence of abnormal secretions in glands and ductules. These secretions often become thick and viscous, leading to obstruction, distention, and atrophy of ductules and acini in both serous and mucous glands. The way in which inactivation of the CFTR chloride channel in epithelial cells leads to this inspissation of secretions and its sequellae is not understood.

Production of mice. A gene equivalent to the human CFTR gene has been identified in mice (8). As reported previously, we and others have inactivated the murine CFTR gene in embryonic stem (ES) cells by targeted insertion of a neomycin gene (9, 10). The disrupted CFTR gene in our targeted cell lines contains an in frame stop codon in the coding sequence of exon 10 (9), and we have designated this mutation as S489X. This gene should give rise to a truncated gene product similar to that seen with several types of human CF mutations. In humans, this type of mutation results in a severe phenotype, similar to that caused by the more prevalent ΔF508 mutation (11).

Because mice generated from our original targeted cell lines failed to transmit the ES cell genome to offspring, we performed additional electroporations and used the same protocol and construct. Typically, E14TG2a cells (about 1×10^7) (12) were subjected to electroporation with the previously described targeting vector, CFneo², and selected in the presence of gancyclovir and neomycin. Colonies were screened with the use of the polymerase chain reaction (PCR) in pools of ten as described (9). In one of these experiments, four targeted cell lines were obtained. The targeting frequency in this experiment was 1 in 300,

much higher than the frequency of 1 in 2500 that we previously reported for targeting with this construct. This increased efficiency was probably due to an increase in the ratio of targeted to nontargeted integration, which, for reasons that remain unclear, often varies between experiments. This explanation is supported by the fact that a control electroporation, performed in parallel with a construct designed to target the hprt locus, gave a targeted to nontargeted ratio of 1:1, ten times higher than that routinely found for this hprt construct.

Three of the four newly generated targeted cell lines were injected in the blastocoele cavity of C57BL/6 embryos and transferred to B6D2 pseudopregnant foster mothers. Offspring showing more than 10 percent chimerism were mated to B6D2, C57BL/6, or BALB/C mice. Transmission of the ES cell genome of chimeras to their offspring was initially determined by examination of coat color. Offspring from two clones, 45-24 and 45-66, transmitted the targeted genome to the next generation. Of the 72 chimeras generated from cell line 45-24, six males transmitted the ES cell genome to their offspring. Of the 38 chimeras generated with cell line 45-66, ten males and four females transmitted the ES cell genome. The S489X mutation was detected by PCR analysis of tail DNA in approximately 50 percent of the offspring that received the ES cell genome. We refer to animals heterozygous for the S489X mutation as CFTR(+/−). Similarly, animals that are homozygous for the normal CFTR gene or for the S489X mutation are referred to as CFTR(+/+) or (−/−), respectively.

Transcription of the CFTR gene after homologous integration of our targeting construct should yield a mRNA that diverges from the normal CFTR mRNA at codon 488 of exon 10 (9). In order to verify that the targeted CFTR allele did give rise to such an altered message, we performed ribonuclease protection assays on total RNA isolated from the colons of CFTR(+/+), (+/−), and (−/−) mice (Fig. 1A).

The protection assay revealed that the CFTR(−/−) animals no longer synthesize a normal CFTR mRNA. The altered size of the fragment protected by the RNA from these animals was consistent with interruption of the normal CFTR transcript at the predicted location. The level of normal CFTR mRNA in CFTR(+/−) animals was reduced to about 50 percent relative to that observed in (+/+) animals. In contrast, the amount of transcript derived from the targeted gene, relative to the normal transcript in (+/+) animals, was only 5 to 10 percent in (+/−) animals and only 1 to 2 percent in (−/−) animals. The decreased amount of the altered transcript, relative to the normal transcript, in heterozygous ani-

J. N. Snouwaert, K. K. Brigman, A. M. Latour, R. C. Boucher, and B. H. Koller are with the Department of Medicine, University of North Carolina at Chapel Hill, Chapel Hill, NC 27599–7020.
N. Malouf and O. Smithies are with the Department of Pathology, University of North Carolina at Chapel Hill, Chapel Hill, NC 27599–7525.

*To whom correspondence should be addressed.

mals was probably due to decreased mRNA stability caused by loss of normal polyadenylation or other stabilizing signals. The small amounts of the altered transcript in CFTR(−/−) animals relative to those in heterozygotes is probably caused by loss of cells expressing the targeted CFTR in the damaged intestinal lining of (−/−) animals (see below).

Growth and development. Mice heterozygous for the S489X mutation were mated, and the numbers of offspring in the resulting litters were recorded. Deaths were recorded and, when possible, the genotypes of the dead animals were determined by PCR analysis of tail DNA. Between 5 and 10 days after birth, surviving pups were weighed, and tail DNA was prepared for determination of genotype by PCR.

Of the offspring born to heterozygotes, 182 survived long enough for determination of genotype by PCR analysis of tail DNA. Nineteen percent of the surviving animals, rather than the expected 25 percent, were CFTR(−/−). However, 30 animals died before a DNA tail preparation could be obtained. Some body parts were found for 23 of these animals, and 12 of these were CFTR(−/−). If a similar proportion of the dead animals that were not recovered had the CFTR(−/−) genotype, then the proportion of genotypes represented at birth becomes 24 percent CFTR(−/−), 49 percent CFTR(+/−), and 27 percent CFTR(+/+). These numbers do not deviate significantly from the expected Mendelian ratio of 1:2:1. It is therefore unlikely that the mutation has any effect on survival to birth of the CFTR(−/−) animals.

A different picture emerges when perinatal survival is examined (Fig. 2). As can be seen, many deaths of CFTR(−/−) animals occurred during the first 5 days of postnatal development, but most of the survivors were still alive at around 20 days after birth. However, during the week after weaning, most of these surviving CFTR(−/−) mice died. Very few lived beyond 30 days, with only one animal to date having survived past 40 days. No difference was seen in the survival of male or female CFTR(−/−) animals. The number of surviving heterozygotes was slightly lower than expected, although there is no evidence to date that this is related to the CFTR(+/−) genotype.

A few offspring obtained from the heterozygote matings showed severe runting at birth, and in most cases these runts proved to be CFTR(−/−) by DNA analysis. Virtually all had weights lower than their normal littermates by the time their tail DNA was sampled at 5 to 10 days of age and, on average, they remained 10 to 50 percent smaller throughout life. However, a few CFTR(−/−) animals maintained a relatively normal body weight until just before death.

As noted above, chimeras were mated to three different strains of mice to obtain the heterozygous parents of CFTR(−/−) mice. There was no obvious correlation between the genetic background of the CFTR(−/−) animals and the age of death or the severity of pathological changes described in the following sections. However, it is still necessary to develop inbred strains containing the S489X mutation to ascertain what affect strain background has on the phenotype of CFTR(−/−) animals.

Intestinal tract. The importance of CFTR for the normal function of the gastrointestinal tract is suggested by high levels of detectable CFTR expression in human intestine and in cell lines derived from human intestine (1). To determine whether this is also true in the mouse, we used ribonuclease protection assays to examine expression of CFTR in various portions of the gastrointestinal system of mice. High levels of CFTR mRNA were detected in the duodenum, jejunum, ileum, cecum, and colon (Fig. 1B), although expression was relatively low in the esophagus and stomach (Fig. 1D, lanes 3 and 4).

In animals that died between 12 and 40 days after birth, death was, in most cases, preceded by loss of weight concomitant with abdominal distention and awkward gait. Of 22 CFTR(−/−) animals that died during this period, 19 had severe intestinal

obstruction and one showed distention of the intestine, although no obvious obstruction was present. In the remaining two animals, decomposition of the carcass prevented determination of the cause of death. In animals with severe obstructions, distention of the proximal segments of the intestine and narrowing of the colon were observed (Fig. 3, A and B). The intraluminal obstruction consisted of a putty-like mass that appeared to be composed of a mixture of mucus and fecal material. In many cases, fecal material was evident in the peritoneal cavity, indicating rupture of the intestine. In other cases, fecal material was evident only on histological examination of the mesentary. By far the most common site of obstruction in animals dying just after weaning was the ileum (Fig. 3A). However, in animals that died more than a few days after weaning, obstruction of the large intestine was more common (Fig. 3B). In two animals, the obstruction of the intestinal tract was accompanied by evidence of a healed rupture surrounded by fibrous tissue, which formed adhesions between several loops of the intestine. Yellow fecal pellets, presumably formed during perinatal life, were still present in the abdominal cavity.

The cause of death of animals that died during the perinatal period was difficult to assess because (i) carcasses were often partially or completely consumed by the moth-
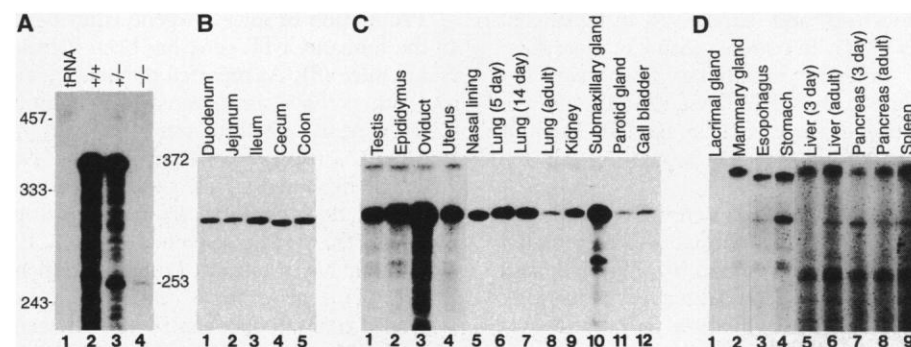

Fig. 1. Ribonuclease protection assays of CFTR mRNA. For all protection assays, total cellular RNA was extracted with a commercially available reagent (RNAzol B, Tel-test) as directed. A ^{32}P-labeled RNA probe containing sequences complementary to exons 9 and 10 of the normal murine CFTR transcript was prepared, and assays were done on 40 μg of RNA from appropriate tissues (25). The same probe preparation was used for each of the samples shown. (**A**) Expression of CFTR mRNA in CFTR (+/+), (+/−), and (−/−) mice. Lane 1 is a negative control reaction carried out on 40 μg of yeast tRNA. Reactions in lanes 2 to 4 were carried out on total colon RNA from animals with the indicated genotypes. Numbers at the right indicate the expected size of protected fragments in base pairs. The CFTR mRNA transcribed from the normal allele should protect a 372-bp fragment, while the transcript from the targeted allele should protect a 253-bp fragment. The gel was autoradiographed for 16 hours, and lanes 2 and 3 were intentionally overexposed to allow visualization of the 253-bp band in lane 4. Sizes of RNA markers (base pairs) are shown on the left. (**B**) Assays on total RNA from tissues of normal mice that express high levels of CFTR mRNA. The gel was autoradiographed for 1.5 hours. (**C**) Assays on total RNA from tissues expressing moderate amounts of CFTR mRNA. Gels were autoradiographed for 16 hours. (**D**) Assays on RNA from tissues of normal mice expressing low levels of CFTR mRNA. Gels were autoradiographed for 5 days. The arrowheads indicate the position of the fragment protected by the normal CFTR transcript. Protected fragments at other positions, especially apparent in (D), are background bands, which are also present in tRNA controls after extended autoradiography. The background band with highest molecular size is residual undigested probe.

er; (ii) postmortem changes were often present before the tissues could be fixed; and (iii) higher death rates occur at this age among normal animals so that more carcasses had to be examined to determine whether death was actually due to the CFTR(−/−) genotype and was not incidental. Despite these difficulties, examination of CFTR(−/−) animals that died in the week after birth did reveal evidence of intestinal complications, including dark fecal material in the intestine, fecal material in the peritoneal cavity, and visible perforation of the intestine.

The actual cause of death in most of the animals with intestinal obstruction was most likely peritonitis in that they presented with an acute inflammatory infiltrate throughout the peritoneal cavity, thymic involution, and hypocellularity of the spleen. The spleen and thymus in all CFTR(−/−) animals killed before developing intestinal obstructions were normal.

The types of intestinal obstructions observed in our CFTR(−/−) mice closely resemble many of the perinatal signs described in early studies of human CF patients. The first manifestation of CF in humans is often meconium ileus, a condition in which newborn infants fail to pass meconium (13, 14). The ileus is caused by obstruction of the ileal lumen by a viscid, sticky meconium mass, near the ileocecal valve. In some cases, neonatal obstruction may result from improper repair of the gut and mesentary after perforation of the distended intestine in utero (15). Small bowel obstruction has also been described beyond the newborn period and is referred to as meconium ileus equivalent (16).

To determine whether any gross intestinal abnormalities were present in CFTR(−/−) mice before intestinal obstruction, animals were killed while apparently still healthy (before loss of weight). In these cases the intestine appeared indistinguishable from that of CFTR(+/−) or (+/+) littermates with the exception of the cecum. In normal mice, the cecum is a large sacklike structure, whereas in CFTR(−/−) mice i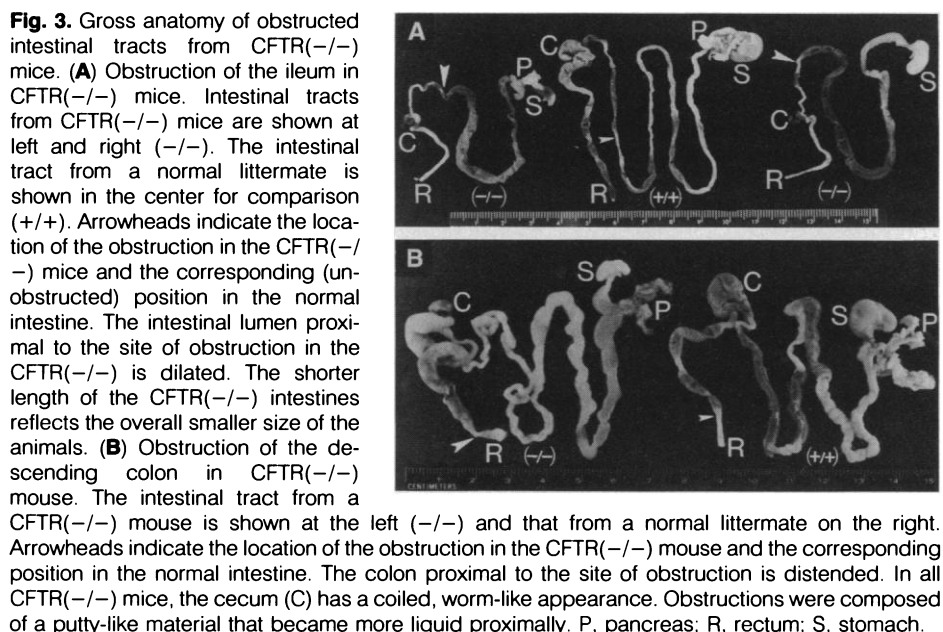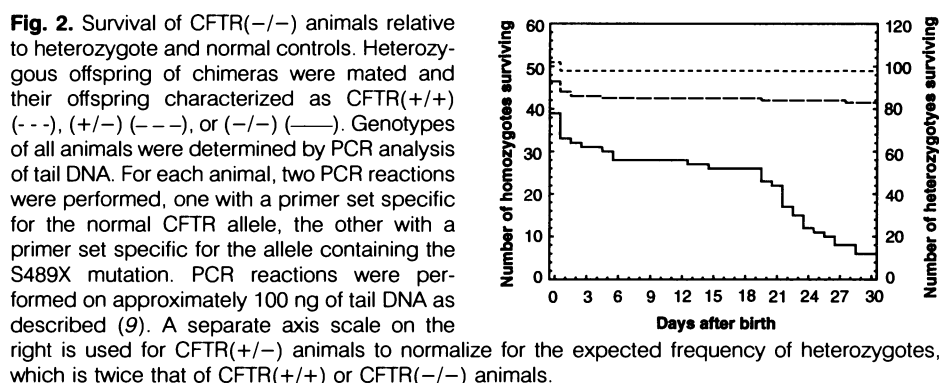t was coiled and worm-like in appearance. The lumen of the cecum of CFTR(−/−) animals was narrowed and partially or completely impacted with hard, sticky fecal pellets.

A possible counterpart to the abnormal cecum observed in CFTR(−/−) mice has been reported in human CF patients. The portion of the cecum that branches from the main track of the intestine differs significantly in its morphology between mice and humans. It is a relatively substantial pouch in mice, while in humans it is a small diverticulum, the vermiform appendix. Several conditions involving the appendix have been reported in human CF patients, including appendiceal abscess and nonfilling appendix due to obstruction by inspissated secretions. A retrospective autopsy review (17) revealed that in 49 of 51 CF patients the mucosa of the appendix was hyperplastic and the mucosal glands were distended with eosinophilic secretions.

Serial histological examinations throughout the intestinal tract provided insight into the cause of obstruction in our animals. Examinations included four CFTR(−/−) animals that died with obstructions in the ileum and two animals with obstructions in the colon. The most dramatic histological changes were present in the crypts of Lieberkuhn, the tubular glands in the mucosa of the small and large intestines. The severity of pathological changes in the crypts followed a proximal to distal gradient, with the mildest changes affecting the duodenum and the most extreme affecting the ileum and colon (Fig. 4, A to F). In the segments of the intestine proximal to the obstruction, inspissated eosinophilic secretions were usually confined to the region at the base of the crypts. However, the changes in the ileum distal to the obstruction included dilation of crypts and formation of concretions and cast-like structures that extended the entire length of the crypts and villi (Fig. 4, C and D). In many cases, the crypts and their associated villi were almost completely destroyed. Distended crypts containing increased amounts of mucus were also present in the ileum and colon of CFTR(−/−) animals without intestinal obstructions (Fig. 4B), indicating that the described changes are not secondary to the distress caused by ileus.

The importance of CFTR for normal function of the crypts of Lieberkuhn is supported by the findings of a previous study that the principal site of CFTR expression in rat intestine is the crypt of Lieberkuhn, with levels of CFTR mRNA decreasing gradually as the cells differentiate and migrate from the crypt to the villus (18).

One feature of the intestinal tract that often shows histological alterations in human CF patients is the Brunner's glands (19), submucosal mucoid-secreting glands of the first part of the duodenum. These glands often show dilation of the lumen,

Fig. 2. Survival of CFTR(−/−) animals relative to heterozygote and normal controls. Heterozygous offspring of chimeras were mated and their offspring characterized as CFTR(+/+) (- - -), (+/−) (− − −), or (−/−) (——). Genotypes of all animals were determined by PCR analysis of tail DNA. For each animal, two PCR reactions were performed, one with a primer set specific for the normal CFTR allele, the other with a primer set specific for the allele containing the S489X mutation. PCR reactions were performed on approximately 100 ng of tail DNA as described (9). A separate axis scale on the right is used for CFTR(+/−) animals to normalize for the expected frequency of heterozygotes, which is twice that of CFTR(+/+) or CFTR(−/−) animals.

Fig. 3. Gross anatomy of obstructed intestinal tracts from CFTR(−/−) mice. (**A**) Obstruction of the ileum in CFTR(−/−) mice. Intestinal tracts from CFTR(−/−) mice are shown at left and right (−/−). The intestinal tract from a normal littermate is shown in the center for comparison (+/+). Arrowheads indicate the location of the obstruction in the CFTR(−/−) mice and the corresponding (unobstructed) position in the normal intestine. The intestinal lumen proximal to the site of obstruction in the CFTR(−/−) is dilated. The shorter length of the CFTR(−/−) intestines reflects the overall smaller size of the animals. (**B**) Obstruction of the descending colon in CFTR(−/−) mouse. The intestinal tract from a CFTR(−/−) mouse is shown at the left (−/−) and that from a normal littermate on the right. Arrowheads indicate the location of the obstruction in the CFTR(−/−) mouse and the corresponding position in the normal intestine. The colon proximal to the site of obstruction is distended. In all CFTR(−/−) mice, the cecum (C) has a coiled, worm-like appearance. Obstructions were composed of a putty-like material that became more liquid proximally. P, pancreas; R, rectum; S, stomach.

flattening of cells of the epithelial lining, and the presence of a stringy eosinophilic secretion. In one study, hyperplasia of Brunner's glands was reported in 82 percent of cases with meconium ileus (19). Unlike humans, in whom Brunner's glands are found throughout the duodenum, mice have only one Brunner's gland near the pylorus. In each of three CFTR(−/−) animals examined that died with intestinal obstructions, most of the gland was de-

stroyed, and the lumens of many of the remaining ducts were distended.

Pancreas. The first noticeable histological change in humans with CF is often dilation of pancreatic acini and the presence of eosinophilic material in pancreatic ductules (20). We were able to detect similar changes in only two of five CFTR(−/−) animals examined. In these animals, one or two lobes contained some enlarged acini, a number of which con-

tained eosinophilic material.

In general, dramatic alterations in morphology were not evident upon gross inspection of the pancreas in CFTR(−/−) mice, although it was often smaller and paler than in normal controls. However, because the mouse pancreas is a diffuse organ, with one arm branching through the mesentary and attaching to the descending colon, its apparent size is often influenced by the amount of fat in the mesentary. It is
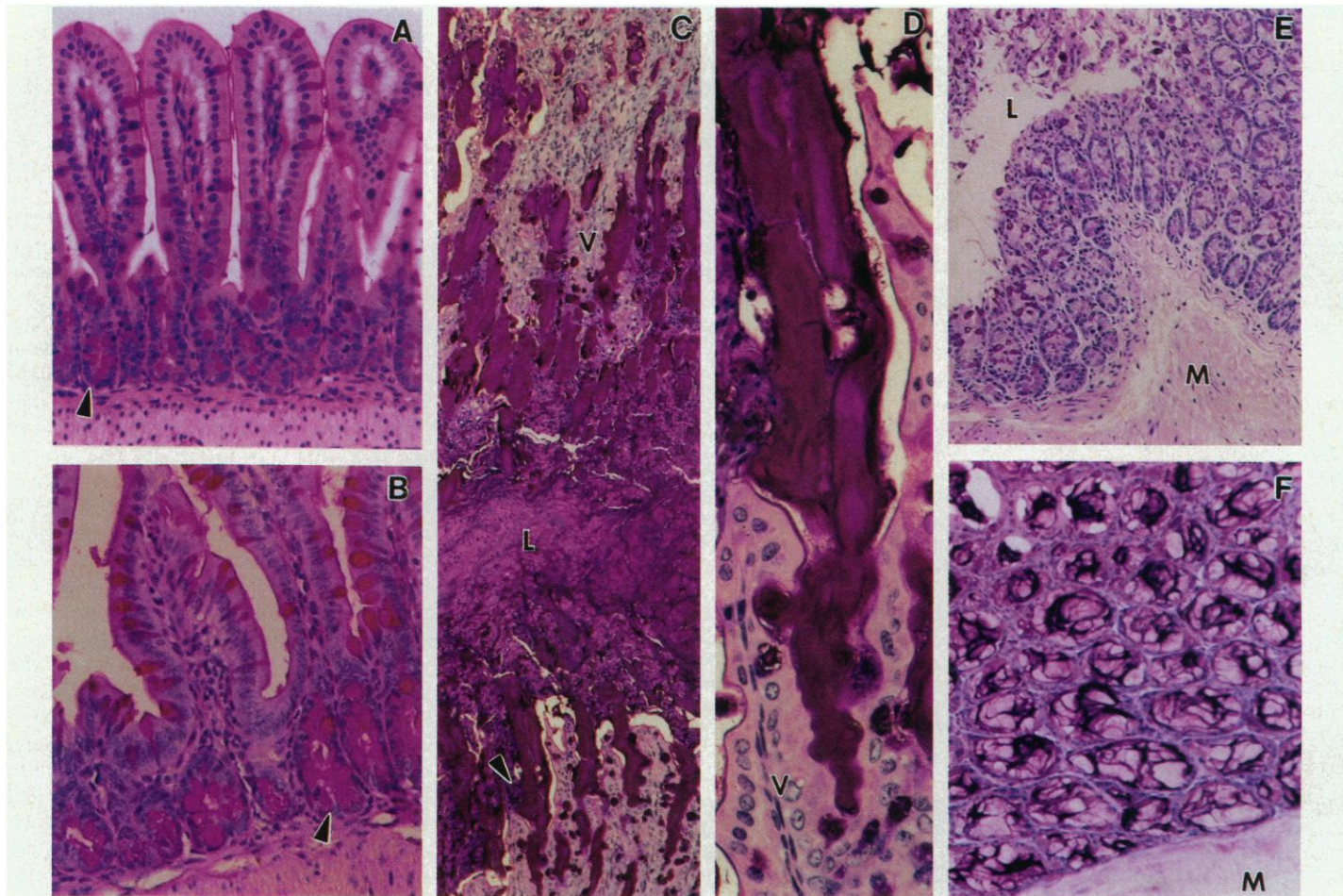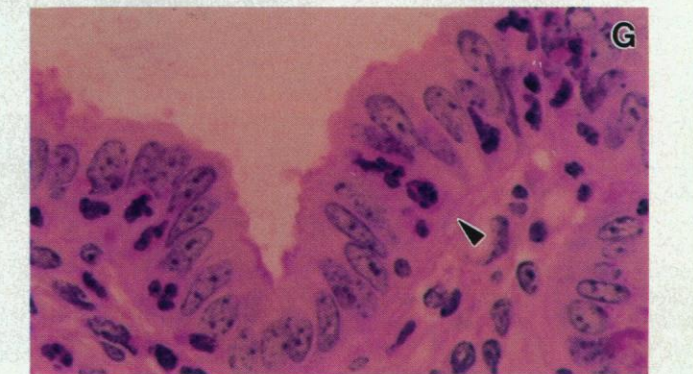

Fig. 4. Histological changes in the intestine and gallbladder of CFTR(−/−) mice. Tissues were fixed in phosphate buffered formalin (pH 7.2), embedded in methacrylate, and cut at a thickness of 4 to 6 nm. Sections were stained with periodic acid Schiff (PAS) and haematoxylin, and counterstained with eosin. The ileum from a normal mouse (**A**) is compared to that of a CFTR(−/−) litternate without intestinal obstruction (**B**). The section from the CFTR(−/−) mouse reveals an increase in the number of goblet cells in both villi and crypts. Distention of the crypts is also evident. The location of the crypts is indicated by the arrowheads. In a longitudinal section of the ileum from a CFTR(−/−) mouse that died with an intestinal obstruction (**C**), markedly dilated crypts, filled with mucus, can be seen extending into the stems of the villi (V). The lumen (L) of the ileum contains mucus and necrotic material. (**D**) Higher magnification of the area indicated by the arrow in (C) reveals laminated concentric concretions formed by accumulation of mucous (magentaPAS staining) in the crypt lumens. A section from the colon of a normal animal (**E**) is compared to a section from the colon of a CFTR(−/−) mouse (**F**), which demonstrates extensive dilation of mucous glands with consequent flattening of the epithelial lining. The lumens of some of the dilated glands also contain mucous concretions. The sections in (E) and (F) are shown at identical magnifica-

tion. M, muscularis. A section of the gallbladder from a CFTR(−/−) animal (**G**) that appeared healthy when killed shows numerous polymorphonuclear cells infiltrating the mucosa. Final magnifications: (A), 200×; (B), 200×; (C), 100×; (D), 400×; (E), 100×; (F), 100×; and (G) 600×.

therefore possible that the apparent changes in the pancreas of CFTR(−/−) animals were merely secondary to poor health brought on by intestinal obstruction.

The relative lack of pathological changes in the pancreas of CFTR(−/−) mice suggests that CFTR may play a smaller role in normal pancreatic function in mice than in humans. This is consistent with the relatively low levels of CFTR mRNA that we observed in the pancreas of normal mice (Fig. 1D, lanes 7 and 8). Although CFTR mRNA is expressed at high levels in human pancreas (1, 21), we were barely able to detect the CFTR transcript by ribonuclease protection assay in the pancreas of both 3-day-old and adult normal mice. Detection of the CFTR transcript in mouse pancreas required exposure of autoradiograms for 5 days, in comparison to approximately 15 minutes required for detection of expression in intestinal tissue.

Liver and gallbladder. Pathological changes in both the liver and gallbladder have been documented in humans with CF. It has been reported that CFTR mRNA is expressed at low levels in human liver (1), and we found a similar situation in normal mature mice (Fig. 1D, lane 6) although we did not detect CFTR mRNA in 3-day-old

liver (Fig. 1D, lane 5). We found higher levels of CFTR expression in the gallbladder (Fig. 1C, lane 12) than in liver.

The major pathological change seen in the livers of humans with prolonged CF is focal biliary cirrhosis (7). Estimates of the percentage of CF patients affected by this condition range between 14 and 43 percent, and its prevalence increases with age (15). Examination of CFTR(−/−) mice to date has revealed no such lesions, although extension of the average lifespan of these animals may be necessary before such changes become evident.

Alterations in the gallbladder of human CF patients include hypoplasia, a content of thick mucus, and calculi (7, 15). Postmortem examination of CFTR(−/−) mice often demonstrated extremely distended or ruptured gallbladders, and, in one case, this organ was filled with black bile, which had also leaked into the surrounding tissues. In CFTR(−/−) animals with intestinal obstructions, histological examinations showed almost complete destruction of the gallbladder wall with some polymorphonuclear cells present. In CFTR(−/−) animals killed while apparently healthy, the infiltration of polymorphonuclear cells throughout the entire wall of the gallbladder suggested an

ongoing inflammatory process (Fig. 4G).

Respiratory tract. Although pulmonary disease is at present the most life-threatening clinical manifestation of human CF, most evidence indicates that the lungs of the human CF newborn are normal. Abnormal airway secretions appear in the first weeks of life. Chronic bacterial infection is acquired in the first few years of life, perhaps preceded by a viral infection that generates inflammation of the airways (22). The earliest morphologic change in the airways of human CF patients is dilation of submucosal gland ducts and acinar structures (23). Later, evidence of mucus obstruction of small airways and goblet cell hyperplasia can be detected. These are accompanied by obstruction of small airways, which is the earliest functional abnormality in the lung (24).

As we described above, our CFTR(−/−) mice die early in life of gastrointestinal obstruction, and not of pulmonary infections. Analysis of mRNA from the respiratory tracts of normal mice reveals that CFTR mRNA is expressed at moderate levels in the mouse nasal mucosa and in the lung (Fig. 1C, lanes 5 to 8), as is also the case in humans (1, 18).
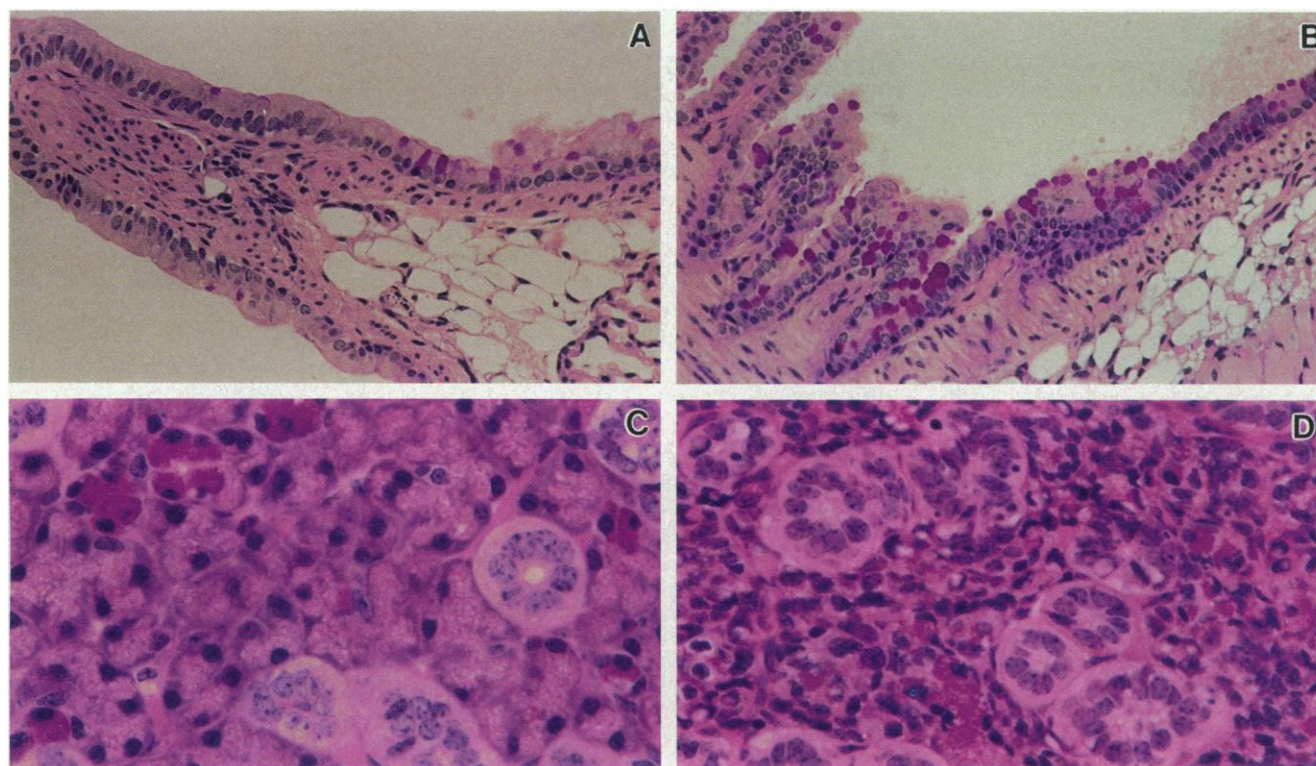
Some of the most striking pathology of

Fig. 5. Sections of lungs showing proximal airways of normal (**A**) and CFTR(−/−) (**B**) mice reveal patches containing increased numbers of goblet cells in the CFTR(−/−) animals. Goblet cells can be identified by the magenta staining of mucous granules. A comparison of sections of the submaxillary glands from normal (**C**) and CFTR(−/−) (**D**) mice demonstrates extensive atrophy of the gland parenchyma in the CFTR(−/−) animal. The atrophy involves predominantly the serous cells of the gland, which have lost the usual vacuolar appearance seen in the normal submaxillary gland. Because of injury to the parenchyma, the gland from the CFTR(−/−) animal appears hypercellular in comparison to the control, which is viewed at the same magnification. The apparent density of ducts in the CFTR(−/−) specimen is also increased for the same reason. Final magnifications: (A), 100×; (B), 100×; (C), 400×; and (D), 400×.

the respiratory tract of the CFTR(−/−) animals was observed in the nasal sinuses, where there was marked atrophy of serous gland tissue in the dorsolateral sinus. In the oldest CFTR(−/−) animal examined to date, which died at 5 weeks, squamous metaplasia was observed in the trachea. Morphologic evaluation of glands in the nasal mucosa and proximal trachea of the CFTR(−/−) mice revealed evidence for dilation of ducts, although no acinar hyperplasia was observed, and no mucous plugs were detected in the airway lumens. While goblet cells have not generally been reported as being present in the airways of normal mice, we observed these cells scattered throughout the proximal airways of both controls and CFTR(−/−) animals. In addition, we observed patches containing numerous goblet cells in the proximal airways of 5 of 7 CFTR animals (Fig. 5B). No such patches were present in the 5 healthy control animals examined (Fig. 5A). No bacteria were detected in airways by histological staining with Brown and Brenn stain, and no polymorphonuclear infiltration of airway walls was observed in five different CFTR(−/−) animals examined.

Reproductive tract. Approximately 95 percent of male CF patients are infertile due to abnormalities of the reproductive tract, which include aspermia, hypoplastic and aplastic epididymal ducts, and complete absence of sperm transport system. These changes have been attributed to obstruction of the genital tract with inspissated secretions at an early age of development (7).

In rats, expression of CFTR mRNA in the testis has been shown to be regulated during the cycle of the seminiferous epithelium (18). As expected from these findings, we found that normal mice express relatively large amounts of CFTR mRNA in both testis and epididymus (Fig. 1C, lanes 1 and 2). However, in the CFTR(−/−) males examined, we found no major abnormalities of the reproductive organs on gross or histological examination. One CFTR(−/−) male that survived to maturity has fathered three litters of offspring, and a second impregnated a female prior to his death resulting from intestinal obstruction.

Decreased fertility has also been reported for human females with CF (7). Consistent with results from human females, we found a relatively high expression of CFTR mRNA in the uteri of normal mice (Fig. 1C, lane 4), and even higher expression in the ovi-

ducts (Fig. 1C, lane 3). A successful mating of one CFTR(−/−) female that survived to maturity did not result in pregnancy.

Salivary glands. In human CF patients, the pathology of the submandibular, sublingual, and submucosal glands include dilated ducts, inspissated secretions, and atrophy of acini (15). In normal mice, we found relatively high levels of expression of CFTR mRNA in the submaxillary gland and moderate levels in the parotid gland (Fig. 1C, lanes 10 and 11). In the four CFTR(−/−) mice examined, submaxillary glands showed varying degrees of disruption of the serous acini in comparison to normal controls. In two animals, the ducts in the submaxillary gland remained intact (Fig. 5, C and D). In contrast to pathological changes observed in human CF patients, no dilation of ducts or presence of inspissated material in ducts was seen in submaxillary glands from CFTR(−/−) mice.

CFTR(−/−) mice as a model for CF. Our CFTR(−/−) mice demonstrate many pathological changes that are strikingly similar to those observed in human CF. Perhaps the most obvious effect of the CFTR(−/−) genotype was a shortened lifespan, due primarily to complications arising from obstruction of the intestinal tract. The altered function of the intestinal tract, as well as that of other tissues, demonstrated one of the basic features of the human disease, the presence of inspissated secretions in various glands. Pathological changes in the respiratory tract of CFTR(−/−) mice include increased numbers of goblet cells, dilation of gland ducts in the nasal and proximal trachea and destructive changes in the epithelia of the upper airways. By alleviating the intestinal disorders in CFTR(−/−) mice, it may be possible to observe more of the symptoms of human CF, such as pulmonary infection, which often do not manifest themselves until months or years after birth. Our CFTR(−/−) animals were in a pathogen-free environment. The response of these animals to pathogens that commonly cause chronic pulmonary infections in human CF patients has yet to be determined.

REFERENCES AND NOTES

1. J. R. Riordan et al., Science 245, 1066 (1989).
2. J. M. Rommens et al., ibid., p. 1059.
3. J. Barasch et al., Nature 352, 70 (1991).
4. N. A. Bradbury et al., Science 256, 530 (1992)
5. F. Collins, ibid., p. 774.
6. B. Kerem et al., ibid. 245, 1073 (1989).
7. T. F. Boat et al., in The Metabolic Basis of Inherited Disease, C. R. Scriver et al., Eds. (McGraw-Hill, New York, ed. 6, 1989), pp. 2649–2680.
8. F. Tata et al., Genomics 10, 301 (1991).
9. B. H. Koller et al., Proc. Natl. Acad. Sci. U.S.A. 88, 10730 (1991).
10. J. Dorin et al., Transgen. Res. 1, 101 (1992).
11. M. R. Knowles, personal communication.
12. M. Hooper, K. Handy, A. Handyside, S. Hunter, M. Monk, Nature 326, 292 (1987).
13. M. B. Donnison, H. Shwachman, R. E. Gross, Pediatrics 37, 833 (1966).
14. D. H. Anderson, Am. J. Dis. Child. 56, 344 (1938).
15. E. H. Oppenheimer and J. R. Esterly, in Perspectives in Pediatric Pathology, H. S. Rosenberg and R. P. Bolande, Eds. (Year Book, Chicago, 1975), vol. 2, pp. 241–278.
16. P. A. diSant'Agnese, V. S. Hubbard, Cystic Fibrosis, L. M. Taussig, Ed. (Thieme-Stratton, New York, 1984), p. 212.
17. V. P. McCarthy, E. J. Mischler, V. S. Hubbard, M. S. Chernick, P. A. diSant'Agnese, Gastroenterology 86, 564 (1984).
18. A. E. O. Trezise and M. Buchwald, Nature 353, 434 (1991).
19. E. H. Oppenheimer and J. R. Esterly, Arch. Pathol. 96, 149 (1973).
20. S. Farber, ibid. 37, 238 (1944).
21. C. R. Marino, L. M. Matovcik, F. S. Gorelick, J. A. Cohn, J. Clin. Invest. 88, 712 (1991).
22. L. M. Taussig, L. I. Landau, M. I. Marks, Cystic Fibrosis, L. I. Taussig, Ed. (Thieme-Stratton, New York, 1984), p. 115.
23. J. Sturgess and J. Imrie, Am. J. Pathol. 106, 303 (1982).
24. W. W. Fox et al., Pediatrics 54, 293 (1976).
25. To construct a template for preparation of an antisense RNA probe, we prepared a double-stranded fragment containing exons 9 and 10 of the CFTR mRNA, using the polymerase chain reaction (PCR). The template for PCR was generated by reverse transcription of total mouse colon RNA in the presence of random hexamer primers. The PCR fragment containing exons 9 and 10 was cloned into the Sma I site of the cloning vector pBluescript SK(−) to produce the plasmid pCFTR9-10. This plasmid was linearized with Bam HI and transcribed with T3 polymerase in the presence of [α-^{32}P]CTP to produce a 457-bp ^{32}P-labeled antisense RNA probe. Forty micrograms of each sample of each RNA was hybridized with 5 × 10^5 cpm of the labeled probe for 16 hours at 45°C, using standard methods (26). RNase digestion was carried out at 15C for 45 min. Protected fragments were analyzed on 6% acrylamide sequencing gels and autoradiographed.
26. M. Gilman, in Current Protocols in Molecular Biology, F. M. Ausubel et al., Eds. (Wiley, New York, 1989), pp. 4.7.1–4.7.8.